Archives of Environmental Sciences and Environmental Toxicology

Yin L, et al. Arch Environ Sci Environ Toxicol 5: 135.

www.doi.org/10.29011/2688-948X.100135

www.gavinpublishers.com

Research Article

Clogging Simulation and Rainwater Runoff Purification Study of Eco-Type Steel Slag Permeable Concrete

Longlong Yin[1,2], Sheng Zhang[3], Jing Yuan[2,4*], Qianfeng Zhang[1]

[1]Institute of Molecular Engineering and Applied Chemistry, Anhui University of Technology, Ma'anshan, P. R. China

[2]Department of Civil Engineering, Tongling University, Tongling, P. R. China

[3]China MCC17 Group Co., LTD, Ma'anshan, P. R. China

[4]University of Alberta, Edmonton, Canada

[*]**Corresponding author:** Jing Yuan, Department of Civil Engineering, Tongling University, Tongling, 244000, P. R. China

Citation: Yin L, Zhang S, Yuan J, Zhang Q (2022) Clogging Simulation and Rainwater Runoff Purification Study of Eco-Type Steel Slag Permeable Concrete. Arch Environ Sci Environ Toxicol 5: 135. DOI: 10.29011/2688-948X.100135

Received Date: 31 March, 2022; **Accepted Date:** 8 April, 2022; **Published Date:** 12 April, 2022

Abstract

The problems of easy clogging and poor purification effect of rainwater runoff of Steel Slag Permeable Concrete (SSPC) are very common. In this paper, a New Eco-Type of Steel Slag Permeable Concrete (NESSPC) was prepared by adding Filter Material Ceramsite (FMC) and Plant Straw (PS), and the clogging condition and water purification ability of NESSPC were numerically simulated and tested by COMSOL Multiphysics and experiment respectively. The results showed that the clogging depth of NESSPC by oil-stained mud sand, mud sand and clay is 10-35 mm, 15-40 mm, and 40-80 mm respectively. The effect of the coarse sand with particle size of 0.6-1.18 mm on the blocking depth of NESSPC is not significant, nevertheless, as the clogging sand particle size decreases, resulting in an increase in the clogging depth of NESSPC. With the porosity raises, the depth of clogging of NESSPC increases, and the purification effect of NESSPC on COD and NH_3-N in rainwater runoff increases, and the purification effect on SS reduces. The purification effect of NESSPC on rainwater runoff gradually increases as the service life increases. This study gives some new thoughts related to the anti-clogging and rainwater runoff purification mechanism of NESSPC and provides theoretical design method for engineering application.

Keywords: Permeable concrete; Steel slag; Steel slag concrete; Pore clogging; Water purification; Numerical simulation

Introduction

With the rapid development of metallurgical industry, the quantity of steel slag is increasing quickly. A large amount of steel slag not only occupies land and pollutes the environment, but also the heavy metals in steel slag will flow into the ground and pollute the groundwater resources. Therefore, the effective deal with steel slag has been widely concerned [1-7].

A large number of experimental studies and theoretical analysis [8-11] reveal that steel slag has a certain degree of hydration cementation, which can enhance the strength of the cemented filler. The use of steel slag in concrete is feasible and valuable for preserving natural resources, protecting the environment, and generating economic benefits [12-14]. Therefore, Lai [15] analysed the influence of the content of coarse steel slag on the mechanical properties of concrete. The results show that the compressive strength of steel slag concrete increases 5.8% compared with ordinary concrete when the steel slag aggregate content is 50%. Sharba [16] studied the effect of steel slag fine aggregate on the mechanical properties of concrete. Results indicated that steel slag can improve the mechanical properties of concrete, and the mechanical properties of concrete are the best when the steel slag fine aggregate content is 22%. Subathra [17] analysed the durability of steel slag concrete under different exposure conditions. Results revealed that steel slag concrete has stronger acid erosion resistance compared with ordinary concrete, and the absorption coefficient of steel slag concrete is lower than that of conventional concrete under extreme, severe and extreme exposure conditions, which proves that steel slag concrete is suitable for extreme climate conditions. Newman [18] studied the durability of steel slag concrete. Results indicate that, compared with ordinary concrete, steel slag concrete has higher corrosion resistance of sulphuric acid, magnesium sulphate and long-term aging resistance.

Permeable concrete is a kind of environment-friendly pavement material, which can maintain the ecological balance of the city. It can slow down surface subsidence, control rainwater runoff pollution, alleviate urban heat island effect and urban water logging [19-23]. To promote the development of permeable concrete and improve the application of steel slag in pavement engineering, some scholars investigated the properties of Steel Slag Permeable Concrete (SSPC). Runze [24] studied the mix ratio of SSPC. The results revealed that when the water-cement ratio is 0.34, the particle size of fine aggregate is 0.6-2.36 mm, and the particle size of coarse aggregate is 2.36-4.75mm, the strength and permeability of SSPC reach the best, which are 35.6MPa and 3.5×10-2 cm/s, respectively. Wang [25] analysed the influence of steel slag content on mechanical properties of SSPC. The results show that with the increase of steel slag content, the permeability and carbonization resistance of SSPC gradually decrease, while the compressive strength of SSPC gradually increases. Zhang [26] analysed the influence of mineral types on durability of SSPC. The results indicated that with the increase of fly ash, ore powder and steel slag powder content, the wear resistance and frost resistance of SSPC increase gradually. It can be seen from the above that the performance of SSPC satisfies the standard of urban road bearing capacity. Therefore, the SSPC is a broad application prospect.

In practical engineering application, SSPC pavement is easy to fill and blocked by silt particles, which leads to the gradual decrease of seepage capacity of SSPC pavement, and it is difficult to play the original seepage and permeability effect [12,27-29]. At the same time, road rainwater runoff carries many pollutants that, if untreated, seep into the ground, not only damage sensitive ecosystems, but also endanger human health. The existing SSPC has low purification effect on rainwater runoff and cannot filter most of its pollutants [30-32]. The problems of clogging and poor purification of rainwater runoff from SSPC pavement have been investigated by some scholars. However, no good solutions have been found.

In conclusion, to improve the ability of SSPC to prevent clogging and to purify rainwater runoff, a New Eco-Type of Steel Slag Permeable Concrete (NESSPC) was prepared by adding Filter Material Ceramsite (FMC) and plant straw (PS) into SSPC in this paper. In view of the lack of performance and mechanism analysis in literature, the effects of blocking fluids, porosity, and sand gradation on the depth of NESSPC blockage were analysed, as well as the purification effect of NESSPC on COD, SS and NH3-N in rainwater runoff. Based on the results, the anti-clogging mechanism and water purification mechanism of NESSPC are revealed.

Simulations and Experimental

Materials

The materials used are P.O42.5R Portland cement, steel slag, FMC, PS, micro-silica, water-reducing agent and water. The NESSPC with small surface pore and large bottom pore was prepared by a stratified casting method of two kinds of aggregate particle size. The ratio of surface layer to bottom layer was 1:9, and the particle size of steel slag aggregate used in surface layer and bottom layer was 2.5-5 mm and 5-10 mm respectively. The NESSPC is shown in Figure 1. Both FMC and PS are embedded in the bottom aggregate, and the aggregate particle size of FMC is 6-8 mm, and the PS is flat and 0.5-1 mm in length. According to the preliminary mechanical properties experiment [33], when the water-binder ratio is 0.29, FMC content is 8%, PS content is 0.3%, micro-silica content is 10% and water-reducing agent content is 0.3%, the compressive strength of the NESSPC can reach 31MPa and the flexural strength is 4.1MPa, which meet the application standards of permeable concrete pavement [34].

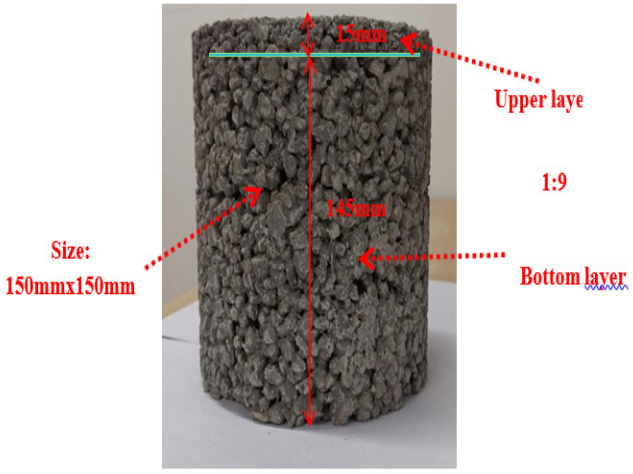

Figure 1: NESSPC forming diagram.

Clogging simulation

Methodology

From the research of Pirnia [35] it is known that the core cause of permeable concrete pavement clogging is the continuous flow of sediment particles with water inside the pore space, which continuously accumulates and results in clogging of the porosity of permeable concrete pavement. The COMSOL Multiphysics finite element software can effectively predict the seepage state of fluids in porous media. Thus, COMSOL Multiphysics was used to numerical simulation of NESSPC plugging using the bidirectional coupling of CFD module and particle tracking module (PTM). Based on Zhou's [36] two-dimensional concrete aggregate random accumulation algorithm. The NESSPC was a composite material that includes aggregates, porosity, and cement, and the NESSPC aggregates were randomly placed using MATLAB software, as shown in Figure 2. At the same time, referring to the DEM numerical simulation results of aggregate size of Ma and Yang [37,38], the particle size of aggregate of surface layer was defined as 2.5mm, 3mm and 5mm, and the particle size of aggregate of

bottom layer was defined as 5mm, 8mm and 10mm, while the particle size of FMC was 6mm and the particle size of PS was 1mm. To simulate the blocking process of NESSPC, the upper and lower parts of the model are set as fluid inlet and outlet, and the left and right sides are set as sliding wall sealing surface. The inlet pressure is 0.14 MPa, and the outlet pressure is 0.01 MPa [39]. The NESSPC aggregate accumulation model was imported into COMSOL to obtain the meshing results, as shown in Figure 3.

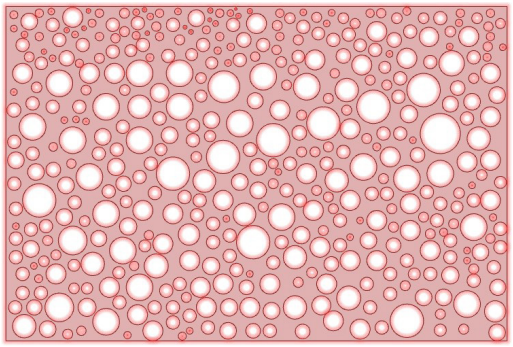

Figure 2: NESSPC aggregate accumulation model.

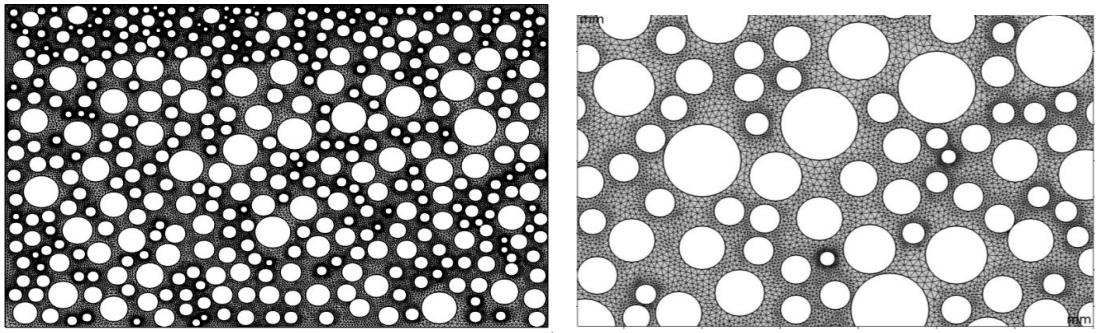

(a) Overall model meshing (b) Local model meshing

Figure 3: NESSPC aggregate model meshing.

Governing equation

The governing equation includes continuous phase and dispersed phase. The fluid in the NESSPC is assumed to be incompressible, isotropic, and the fluid percolation is an isothermal process with a temperature of 293.15K. The continuous equation and the incompressible N-S (Navier-Stokes) equation are used to describe the seepage zone. The continuous equation is shown in Equation 1.

$$\frac{\partial(\delta\rho)}{\partial t}+(\nabla\delta\rho v)=0 \qquad (1)$$

Additional volume forces and porosity are added to the N-S equation to account for the influence of blocking particles in the fluid. The N-S equation is shown in Equation 2-4.

$$\frac{\partial(\rho\lambda v)}{\partial t} + (\nabla\cdot v)(\rho\lambda v) = \theta\nabla^2(\lambda v) - \nabla Q - f_e + \rho\lambda g \quad (2)$$

(3)

$$\frac{\partial\lambda}{\partial t} + \nabla\cdot(\lambda v) = 0$$

$$f_e = \sum_{i=1}^{n} f_b \quad (4)$$

Where, ρ is the fluid density, λ is porosity, ν is fluid velocity vector, θ is fluid dynamic viscosity coefficient θ =η ρ, η is the viscosity of the fluid, Q is pressure, g is gravitational acceleration, f_e is volume force of fluid per unit volume, f_b is volume force of fluid on a single particle, n is the number of particles per unit volume. Similarly, the momentum equation of clogged particles in the fluid also considers the extra volume force when interacting with the fluid, and the mathematical model is shown in Equation 5-6.

$$m\frac{\partial u_k}{\partial t} = f_m + f_b + mg \quad (5)$$

$$\frac{\partial\omega}{\partial t} = \frac{M}{I} \quad (6)$$

Where, u_k is the velocity of the particles in the fluid, m is the mass of the particles, f_m is the sum of the volumetric forces acting on the particles, ω is the angular velocity of the particles, g is the acceleration of gravity, I is the inertial momentum, and M is the moment acting on the particles.

According to Ma [37], the volume force of fluid acting on blocked particles mainly includes drag force, pressure gradient force and other forces. To simplify the calculation formula, the volumetric force on the blocked particles is assumed to include only drag force and pressure gradient force. Therefore, the volumetric force can be calculated as Equation 7-8.

$$f_b = f_d + \frac{3}{4}\pi r^3\nabla Q \quad (7)$$

$$f_d = \left(\frac{1}{2}\rho\pi r^2\right)|v - v_i|(v - v_i)\left(0.63 + \frac{4.8}{\sqrt{Re}}\right)^2 \alpha \quad (8)$$

Where, f_d is the drag force of the fluid, r is the radius of the particle, α is the empirical factor considering porosity, Re is the Reynolds coefficient of the blocked particle, and v_i is the flow velocity of a single particle.

According to the relevant experimental study of Ma [37] and Cui [39], the Reynolds coefficient Re and α can be calculated by the following Equation 9-10. d is the thickness of NESSPC.

$$Re = \frac{d\rho|v - v_i|}{\mu} \quad (9)$$

$$\alpha = 3.7 - 0.65\exp\left[-\frac{(1.5 - \log Re)^2}{2}\right] \quad (10)$$

The CFD module simulates the flow of the fluid, and the PTM simulates the movement of particles in a fluid under the force of gravity, and two-way coupling is performed between both of them. Equation 1-Equation 4 are achieved by CFD module, and Equation 5-Equation 10 are achieved by the PTM. The volume force on the particle is determined by the PTM, the fluid velocity and pressure of each unit is determined by the CFD module. To achieve the blockage simulation of NESSPC.

Material parameters

Three different clogging materials were selected and mixed into clogging fluid for numerical simulation. In the simulation, the density of water is 1000, and the viscosity of water is 0.001pa.s. Based on relevant studies [40-42], the mass ratio of three kinds of blocking fluid was defined. Clay was a mixture of water and clay. Mud sand is a mixture of sand, clay and water, and sand: clay = 1:4; oil-stained mud sand is oil, sand, clay and water, and oil: clay: sand = 1:1:4. (The sand is full-grade sand, as shown in Table 2.) According to the mass ratio of blocking fluid, take 100g blocking material into 2L water. Parameters of three kinds of blocking fluids were obtained through experimental collection, as shown in Table 1.

To simulate the blocking process of NESSPC more accurately, the blocking gravel includes fully graded sand, coarse sand, and fine sand. According to relevant studies [37,43,44], the density, shear modulus and Poisson's ratio of the three gravels are assumed as 2624 kg/m^3, 1×10^{6}pa, and 0.3, respectively. The recovery coefficient, static friction coefficient and sliding friction coefficient between particles are 0.01, 0.5 and 0.21 respectively. The grain size distribution of sand is shown in Table 2.

Parameters	Clay	Mud sand	Oil-stained mud sand
Particle size range (mm)	0.005~0.05	0.05~0.3	0.05~0.3
Density (g× cm^{-3})	1.35	1.63	1.89
Viscosity (Pa ×s)	13.4	17.7	26.3

Table 1: Parameters of blocking fluid.

Note: The viscosity experiment was carried out by GB/T22235-2008 [45]. Density experiment was carried out through GB/T4472-2011 [46].

Particle size(mm)	Fully graded sand (%)	Fine sand (%)	Coarse sand (%)
0.15-0.3	40	30	0
0.3-0.6	35	70	0
0.6-1.18	25	0	100

Table 2: Gravel gradation of blocking sands.

Note: The apparent densities of coarse sand, medium sand and fine sand are 2615 (kg/m^3), 2624 (kg/m^3) and 2695 (kg/m^3) respectively.

Setting of simulated working conditions

To investigate the factors of blockage occurring in NESSPC. The influence of blocking fluid, porosity, and sand gradation on the blocking depth of NESSPC were investigated by the principle of control variable method. Meanwhile, according to the experimental studies of Cui [39] and Lee [47], the water depth of NESSPC road surface is assumed at 150mm, and the horizontal flow speed of the road surface is controlled at 0.2mm/s. The simulated working conditions are shown in Table 3.

Experiment	Porosity (%)	Sand and gravel grading	Blocking material
1	15	Fully graded sand	Mud sand
2	20	Fully graded sand	Mud sand
3	25	Fully graded sand	Mud sand
4	20	Fine sand	Mud sand
5	20	Coarse sand	Mud sand
6	20	Fully graded sand	Clay
7	20	Fully graded sand	Oil-stained mud sand

Table 3: Working condition setting of NESSPC plugging simulation.

Rainwater runoff purification experiment

Polluted water sample configuration

According to the detection data of Erfanul and Thamali [48,49], the main pollutants in urban rainwater runoff are suspended particulate matter (SS), chemical oxygen demand (COD), ammonia nitrogen (NH_3-N), etc., whose concentration exceeds the level V standard of surface water environmental quality. Therefore, the SS, COD and NH_3-N were taken as the characterization indexes of road rainwater runoff pollutants to study the purification effect of NESSPC on rainwater runoff.

Based on relevant studies [50,51], the method of adding chemical reagents to ordinary distilled water was adopted to configure rainwater runoff pollution water samples. The target concentrations of SS, COD and NH_3-N and the usage of corresponding chemical reagents in the experiment are shown in Table 4. The concentration of mixed solutions in rainwater runoff is shown in Table 5.

Indicators ($mg \times L^{-1}$)	COD	NH_3-N	SS
Target concentration	145~270	3~15	260~600
Raw water concentration	210	5	600
Sample	$C_6H_{12}O_6$	NH_4CL	Sedimentary soils

Table 4: Concentration index and corresponding chemical reagents.

Note: $C_6H_{12}O_6$ is a glucose solution, and NH_4CL is a standard solution of ammonia nitrogen.

COD	NH_3-N	SS
(mg × L^{-1})	(mg × L^{-1})	(mg × L^{-1})
200	10	400

Table 5: Contaminant concentration of NESSPC clogging mixed solution.

Experimental program

Experimental investigations by Newman [52] show that the food source of microorganisms in permeable concrete pavement is mainly oil stains. Because, the oil stain can be transformed into a variety of sugar components by the metabolic action of aerobic bacteria and fungi when the oil stain stays in the permeable concrete pavement interior. Thus, the NESSPC containing microorganisms and NESSPC without microorganisms were compared and analysed. The waste oil was sprinkled on the NESSPC, and the NESSPC with the oil was moist environment curing for 56 days. Oil stain curing was used to understand the purification effect of pollutants in rainwater runoff after microbial growth in NESSPC. The experiment scheme is shown in Table 6.

Group	Porosity（%）	With/Without oil stains
G1	15	Non-oil stain caring
G2	20	Non-oil stain caring
G3	25	Non-oil stain caring
G4	15	Oil stain caring
G5	20	Oil stain caring
G6	25	Oil stain caring

Table 6: NESSPC experiment scheme for rainwater runoff.

Experiment Method

In the experiment, SS, COD and NH_3-N were determined by “Gravimetric Method of Suspended Solids in Water Quality” (GB/T11901-1989) [53], “Determination of Water Chemical Oxygen Demand - Dichromate Method” (HJ/828-2017) [54] and “Determination of Ammonia Nitrogen in Water” (HJ/535-2009) [55]. To directly reflect the purification effect of NESSPC on various pollutants in rainwater runoff. The calculation formula of pollutant removal ratio is defined as follows:

$$\upsilon = \frac{C_1 - C_2}{C_1} \times 100\% \qquad (11)$$

Where, υ is the removal ratio of pollutants (%), C_1 is the concentration of pollutants in water (mg/L), C_2 is the concentration of pollutants in water at time t (mg/L), and υ_{COD}、υ_{SS}、υ_{NH-N} are the removal ratios of pollutants COD, SS and NH_3-N respectively.

Results and discussion

Clogging depth

The depth of blockage is an important index to reflect the degree of blockage of permeable concrete. Figure 4, Figure 5, and Figure 6 show the influence of plugging fluids, porosity, and sand gradation on the plugging depth of NESSPC. To reflect the blockage depth of NESSPC more accurately and obviously, the blockage results are represented by the concentration. The red areas in the figs are the main area of NESSPC blockage.

Effects of blocking fluids

The influence of blocking fluids on the blocking depth of NESSPC is shown in Figure 4. Obviously, when the plugging objects are respectively oily-stained mud sand, mud sand and clay, the plugging depth of NESSPC is 10-35mm, 15-40mm and 40-80mm. This indicates that NESSPC is easily blocked by oily-stained mud sand and mud sand, while NESSPC is blocked by clay for a relatively long time. This is mainly because of the wide range of particle size of mud sand. In the process of mud sand moving downward with water flow, the larger particle size can quickly form the skeleton structure in the pores of NESSPC, resulting in the rapid blockage and deposition of fine sand around the skeleton particles. Therefore, the blockage time of mud sand is relatively short. At the same time, oil stains have hydrophobicity and strong viscoelasticity. After oil stains are added, the mud and sand particles easily stick to the hole walls of the NESSPC, forming a serious blockage. Clay has very small particle sizes, so it can flow down with water. Some of the clay sticks to the internal pores of the permeable concrete, forming a loose blocking structure, and some of the clay is pushed out of the permeable concrete by the water. As a result, clay clogs for a longer time. According to the above analysis, oily stained can form a closed and stable blocking structure inside the NESSPC road surface, and the blocking degree is difficult to recover. Furthermore, the clogging structure formed by the small particles such as clay is loose and unstable, and the original permeability function can be restored under human intervention.

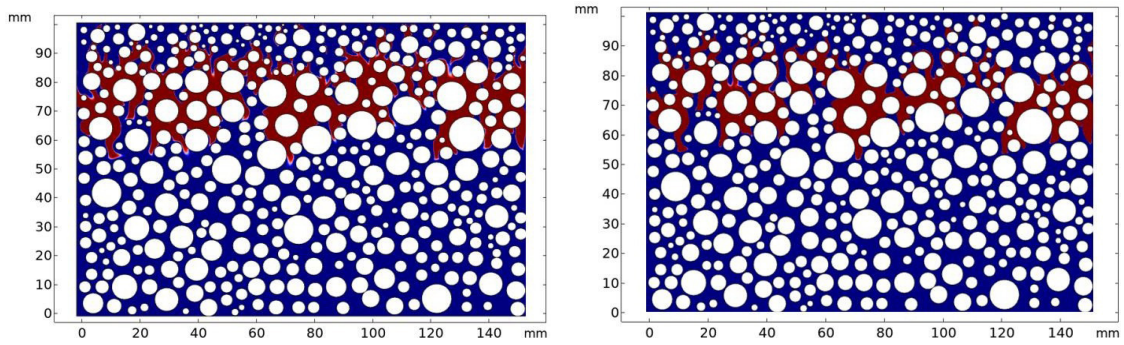

(a) Oily-stained mud sand.

(b) Mud sand.

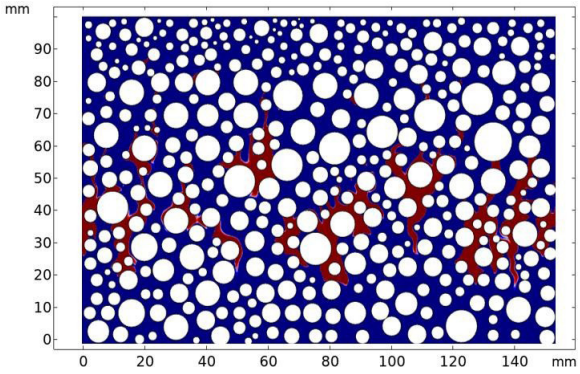

(c) Clay.

Figure 4: Influence of blocking fluids on plugging depth of NESSPC.

Effect of Porosity

The effect of porosity on NESSPC plugging depth is shown in Figure 5. The plugging depth and plugging thickness of NESSPC increases as the porosity increases. This indicates that with the increases of porosity, the amount of sand trapped in the NESSPC increased and the degree of blockage increased. This is mainly because, with the increase of porosity, the pore size and curvature of the connected pores in permeable concrete pavement increase, leading to the decrease of the internal force preventing the flow of particles, and the blocked particles are difficult to form a stable sedimentary structure in the early stage of seepage. Thus, as the porosity increases, the number of blocked particles trapped in the NESSPC increases. According to the above analysis, the greater the porosity of NESSPC, the greater the depth of blockage and the shorter the service life.

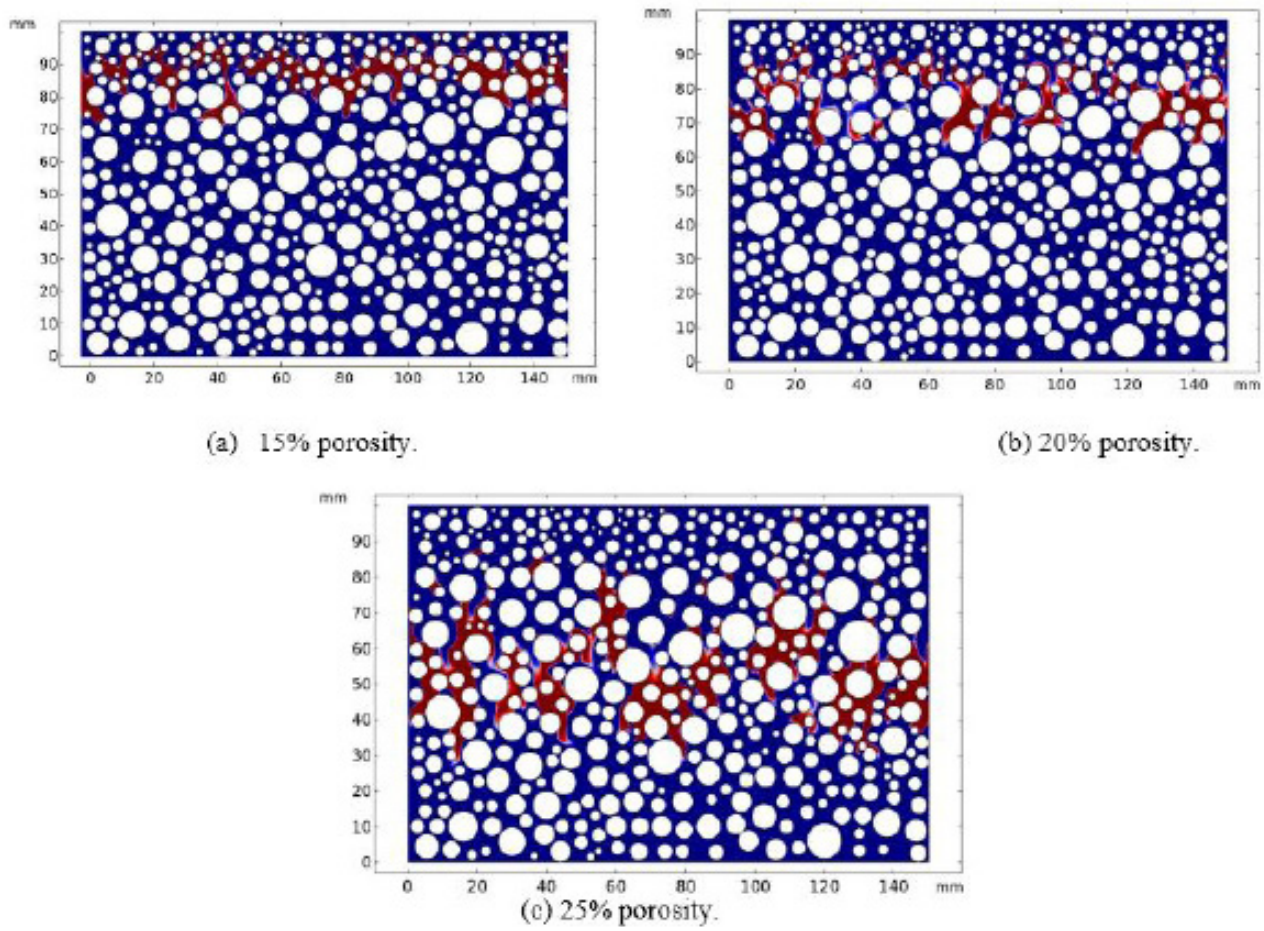

Figure 5: Influence of porosity on plugging depth of NESSPC.

Effects of sand gradation

The influence of sand gradation on the plugging depth of NESSPC is shown in Figure 6. Most of the coarse sand stays at 0-15mm, the fully graded sand stays at 15-40mm depth, and the fine sand can stay at 20-75mm depth. This is mainly because the internal pores of NESSPC are irregular, and the sand with large particle size is easy to form skeleton pore structure on the surface of NESSPC under the action of water flow, which is difficult to move down with water flow. The blockage depth of coarse sand is relatively shallow. Fine sand is easy to migrate to the bottom under the action of water flow, but with the increase of migration depth, the seepage dynamic of sand decreases, resulting in fine sand is easy to stick to the internal pore wall of NESSPC, blocking the connected pores of NESSPC. However, in the downward migration process of fully graded sand, the larger sand particles are easy to form new skeleton particles, leading to the reduction of the pore size around the particles. At this time, the smaller sand particles will rapidly accumulate and settle around the skeleton particles, resulting in blockage. Therefore, the plugging position of fully graded sand is relatively shallow compared with fine sand. According to the above analysis, coarse sand can be quickly deposited in the NESSPC, but the clogging effect is not satisfactory. However, both fine sand and fully graded sand can form stable sedimentary arch structure in NESSPC which causes serious blockage. This is like the experimental results of Kayhanian [56].

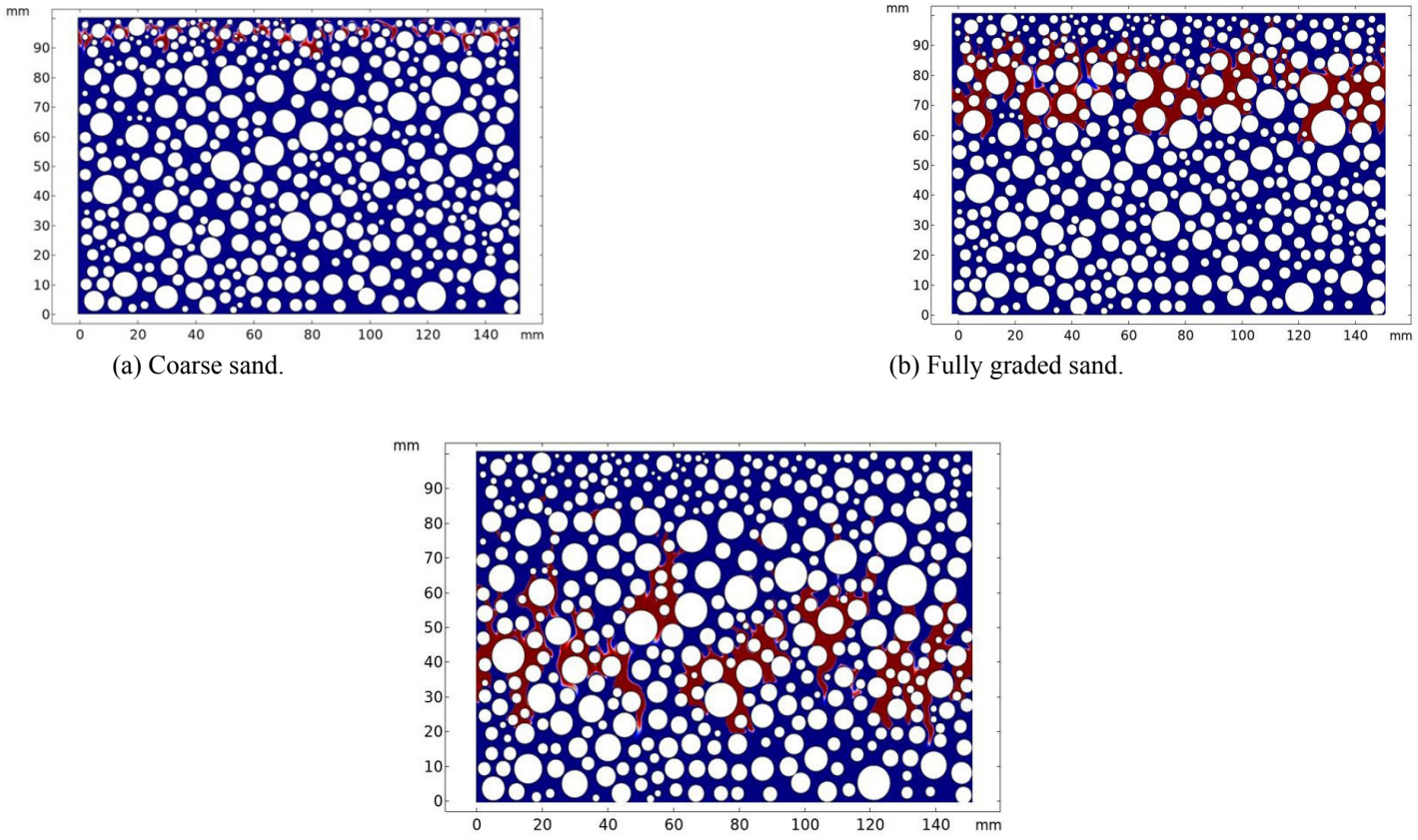

(a) Coarse sand.

(b) Fully graded sand.

(c) Fine sand.

Figure 6: Influence of sand gradation on plugging depth of NESSPC.

The clogging condition of NESSPC was numerically simulated by COMSOL Multiphysics simulation software, and the influence of blocking fluids, porosity, and sand gradation on the clogging depth of NESSPC were analysed, and a consistent conclusion with the corresponding physical test [57] was obtained. The research achievements provide some basis for the prevention and restoration of pore blockage in NESSPC pavements and the optimization of pavement design.

Removal Ratio of Various Pollutants

Figures 7-9 show the influence of NESSPC on the removal ratio of pollutants in rainwater runoff. Where, YZB stands for NESSPC of general maintenance, and YZB stands for NESSPC of oil stain maintenance. The experimental data of porosity obtained from [58,39], standard uncertainties u is $u(\lambda) \le 0.22\%$, the evaluation method refers to [59].

COD Removal Ratio

Figure 7 shows the influence of NESSPC on COD removal ratio in rainwater runoff. The COD removal ratio of NESSPC form rainwater runoff gradually increases as the increase of porosity. After curing with oil stains, the COD removal ratio of NESSPC in rainwater runoff increases, and with the increase of porosity, the increase ratio increases obviously. This is mainly because, with the increase of porosity, the number and thickness of the bonding points between the aggregate of NESSPC decrease, resulting in the increase of the looseness of the internal pore structure, and the thickness of the cement inclusion layer of the FMC reduce. The adsorption capacity of NESSPC to COD in rainwater runoff is enhanced. After NESSPC is cured by oil stains, complex microbial colonies are generated on the surface of ceramic particles inside the NESSPC. Under the condition of oxygen, microorganisms can synthesize COD into cellular substances or catabolize metabolism. Therefore, the COD purification effect of NESSPC is obviously enhanced. In addition, with the increase of porosity, the exposed area of FMC in the NESSPC increases, and after oil curing, the microbial content in the NESSPC increases. Therefore, with the increase of porosity, the COD removal ratio of NESSPC increases significantly.

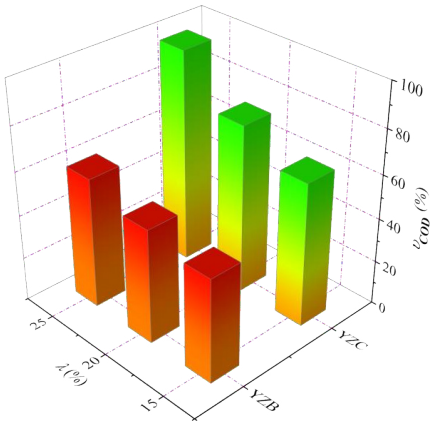

Figure 7: Influence of NESSPC on COD removal ratio in rainwater runoff.

SS Removal Ratio

Figure 8 shows the influence of each NESSPC on SS removal ratio in rainwater runoff. The removal ratio of SS from rainwater runoff by the NESSPC decreases as the increase of porosity. After oil stain curing, the SS removal ratio of NESSPC in rainwater runoff increased obviously. This is mainly because, with the increase of porosity, the pore size and number of connected pores in the NESSPC increase, and the looseness of the accumulation structure formed by suspended particles in the NESSPC pores increases. Under the continuous scouring of water flow, part of SS retained in the NESSPC is easy to wash down and discharged from the NESSPC. Therefore, with the increase of porosity, the removal ratio of SS from rainwater runoff gradually decreases. Secondly, after oil curing, bacteria and fungi and other microorganisms on the surface of the FMC in the NESSPC have high decomposition ability and sedimentation performance, and SS in the rainwater runoff can be adsorbed to the FMC surface, thus improving the removal ratio of SS in the rainwater runoff.

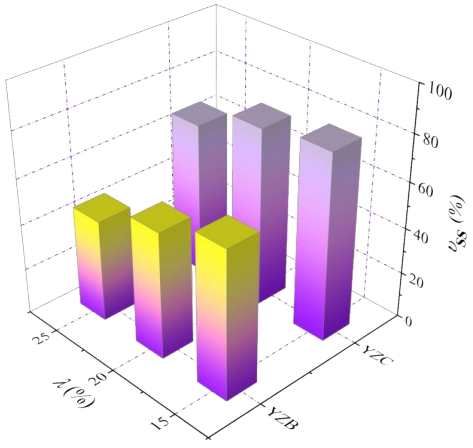

Figure 8: Influence of NESSPC on SS removal ratio in rainwater runoff.

NH_3-N Removal Ratio

Figure 9 shows the influence of NESSPC of each group on NH_3-N removal ratio in rainwater runoff. The removal ratio of NH_3-N from rainwater runoff increases as the increase of porosity. After oil curing, the NESSPC has no obvious effect on the increase of NH_3-N removal ratio in rainwater runoff. This is mainly because, with the increase of porosity, the filling ratio of cement in the NESSPC decreases, leading to the increase of the contact area between FMC and rainwater runoff in the NESSPC, and its adsorption capacity. Therefore, the removal ratio of NH_3-N increases gradually. On the other hand, the nitrogen removal mechanism of microorganisms is mainly through denitrification to transform NO_2--N, NO_3--N into N_2 and NO_2. NESSPC is porous and breathable material, and sufficient oxygen in the NESSPC inhibits the activity of nitrogen oxide reductase, resulting in inhibition of denitrification. Therefore, the removal ratio of NH_3-N from rainwater runoff by NESSPC did not increase significantly after oil stain curing.

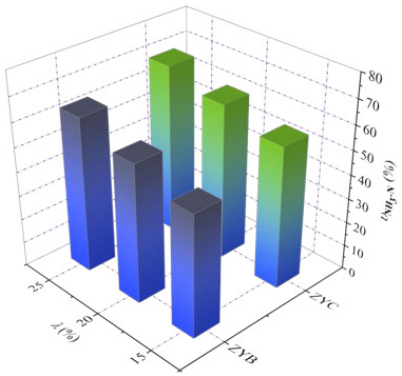

Figure 9: Influence of NESSPC on NH_3-N removal ratio in rainwater runoff.

According to the above analysis, with the gradual increase of porosity, the purification effect of NESSPC on COD and NH_3-N in rainwater runoff gradually increases, while the purification effect on SS gradually decreases. Secondly, with the increase of service life, the number of microbial propagation in NESSPC road surface gradually increases, and the removal effect of pollutants in rainwater runoff gradually increases.

The mechanism analysis of anti-clogging and water purification

Anti-clogging Mechanism

The blocking mechanism of mud and sand particles [60] is mainly the ratio of permeable concrete aggregate particle size to blocking particle size, namely, $\vartheta = d_t / d_s$ where d_t is the aggregate particle size of road surface and d_s is the particle size of blocking particles. When, $\vartheta < \sqrt{3}/(2-\sqrt{3}) \approx 6.46$, the sand particles cannot pass through the surface pores into the road surface, resulting in

many sand particles are blocked out of the road surface, reducing the phenomenon of sediment accumulation and settlement in the internal structure of pervious concrete.

Therefore, the NESSPC with small surface pore and large bottom pore was prepared by a stratified casting method of two kinds of aggregate particle size. The particle size of aggregate on the surface is 2.5-5 mm. Therefore, sand particles with particle size greater than 0.75mm and household garbage are obstructed from the road surface, prolonging the blockage process of the road surface.

On the other hand, FMC and PS were added into the SSPC bottom aggregate. The purpose is to take advantage of the advantages of large specific surface area and strong adsorption capacity of FMC, adsorb the pollutants such as oil stains and bacteria in road rainwater runoff to the surface of FMC, and provide necessary living conditions for the reproduction of microorganisms. SEM morphology of the interface transition zone between aggregate and cement in NESSPC is shown in Figure 10. Obviously, compared with the steel slag-cement interface transition zone, there are many pores and holes in the FMC-cement interface transition zone, which indicates that the incorporation of FMC can significantly improve the adsorption capacity of NESSPC. In addition, there are many micro pores in the interface transition zone, which is conducive to the breeding and propagation of microorganisms. In addition, when the microbial film is generated in NESSPC, the PS that is not evenly wrapped by cement will gradually degrade under the adhesion of the microbial film, so that new microporous structure can be generated in NESSPC, extending the service life of NESSPC road surface.

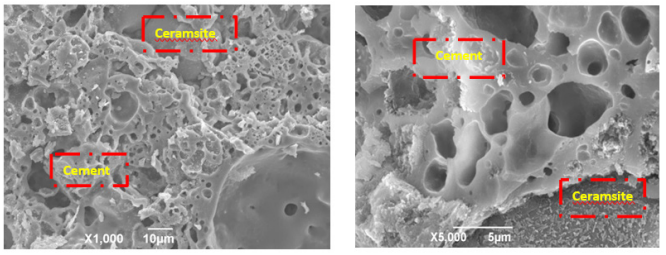

(a) FMC-cement interface transition zone

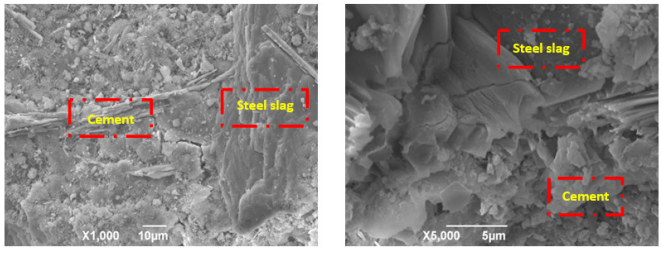

(b) Steel slag-cement interface transition zone

Figure 10: Aggregate - cement slurry interface transition zone.

Mechanism of Water Purification

NESSPC is a new type of pervious concrete material. The defouling method of pervious concrete mainly focuses on three aspects: (1) cement matrix filtration; (2) adsorption of particles of FMC; (3) Microbial degradation and filtration.

Cement Matrix Filtration

Cement matrix is an important part of NESSPC to purify rainwater runoff. This is mainly because the hydration of cement can form silicon compounds, aluminium-iron compounds, and gels, which can transform pollutants such as COD and TP from the dissolved state into solid precipitates.

Therefore, some pollutants in rainwater runoff can be trapped in NESSPC pores. At the same time, there are a large number of microporous structures on the cement matrix, and when it is immersed in water, the microporous structure forms many cement-water critical surfaces, which can promote the dissolution of $Ca(OH)_2$, Al^{3+}, Mg^{2+} and other elements in sewage, and the ion exchange adsorption between these elements and NH_4^+ and PO_4^{3-} in water, so as to achieve the purpose of water purification.

Adsorption of FMC

FMC is one of the most important decontamination components of NESSPC. The surface of FMC is shown in Figure 11. The FMC has large specific surface area, abundant micro pores, strong adsorption capacity and fast microbial reproduction. Therefore, the uniformly dispersed ceramic filter material inside the NESSPC can produce adsorption and filtration effect on suspended particles, heavy metals, NH3-N, COD, and other pollutants.

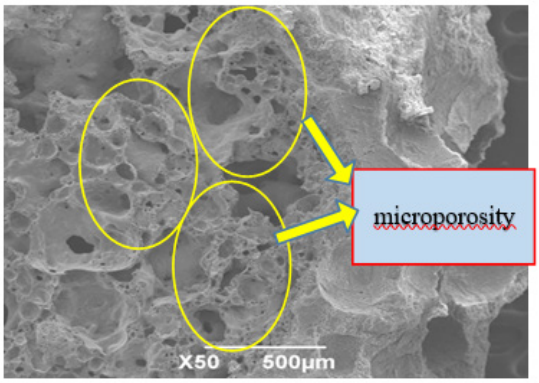

Figure 11: Surface of FMC.

Microbial Degradation and Filtration

According to the analysis of the experiment results, with the increase of time, many microorganisms will grow on the FMC and the surface of PS in the NESSPC, and the microorganisms

take the pollutants in rainwater runoff as nutrients, which greatly enhances the purification ability of NESSPC on rainwater runoff. For example, microorganisms can decompose organic waste in rainwater runoff, while bacteria can oxidize iron sulphide into Fe^{3+} and SO^{2-}, and methanogens can decompose carbonate into methane. Therefore, the microbial colony in the NESSPC plays a core role in the purification of rainwater runoff.

Conclusion

In this paper, a NESSPC was prepared by adding FMC and PS, and the clogging condition and water purification ability of NESSPC were simulated and experimented respectively. The effects of blocking fluid, porosity and sand gradation on the blocking depth of NESSPC and the purification effect of NESSPC on COD, SS and NH_3-N in rainwater runoff were analysed. The following

Conclusions can be drawn

1. NESSPC is easily blocked by mud sand and oil-stained mud sand, while NESSPC is blocked by clay for a relatively long time. The blockage structure formed by oil stain is difficult to recover, while the blockage structure formed by clay is loose and unstable, and the original permeability function can be restored under human intervention.
2. With the increase of porosity, the amount of blocked sand retained in NESSPC gradually increased, and the degree of blockage increased. Coarse sand has little effect on NESSPC blockingeffect, while fine sand and fully graded sand can cause serious blocking effect on NESSPC.
3. With the increase of porosity, the purification effect of NESSPC on COD and NH_3-N in rainwater runoff increases, while the purification effect on SS decreases. The number of microorganisms in NESSPC increased as the increase of service life, and the removal effect of pollutants in rainwater runoff increased gradually. In conclusion, based on numerical simulation and experimental study, the blocking mechanism of NESSPC and its purification mechanism of pollutants in rainwater runoff are explained. This original investigation provides a theoretical basis for the engineering application of NESSPC.

Supplementary Material

Supplementary data associated with this article can be found, in the online version, at application number: 202010766739 .9.

References

1. Shi YM, Du XH, Meng QJ, Song SW, Sui ZT (2007) Reaction Process of Chromium Slag Reduced by Industrial Waste in Solid Phase. J Iron Steel Res 14: 12-15.
2. Sanni E, Puheloinen EM, Kanerva J, Ekroos A, Zevenhoven R, et al. (2010) Co-utilisation of CO_2 and steelmaking slags for production of pure $CaCO_3$-legislative issues. J Clean Prod 18: 1833-1839.
3. Feng H, Yu F, Xie JL, Xie J (2012) Fabrication and characterization of glass-ceramics materials developed from steel slag waste. Mater Design 42: 198-203.
4. Andreas L, Diener S, Lagerkvist A (2014) Steel slags in a landfill top cover-Experiences from a full-scale experiment. Waste Manage 34: 692-701.
5. Jianlong G, Bao YP, Wang M (2018) Steel slag in China: Treatment, recycling, and management. Waste Manage 78: 318-330.
6. Delgado BG, Viana AF, Eduardo F, Paulo M (2019) Mechanical behavior of inert steel slag ballast for heavy haul rail track: Laboratory evaluation. Transp Geotech 20: 100243.
7. Minh VT, Luong NN, Kangkang L, Qiang F, Johir MAH, et al. (2020) Biomethane production from anaerobic co-digestion and steel-making slag: A new waste-to-resource pathway. Sci Total Environ 738: 139764.
8. Alanyali H, Coel M, Yilmaz M (2009) Concrete Produced by Steel-Making Slag (Basic Oxygen Furnace) Addition in Portland Cement. Int J Appl Ceramic Technol 6: 736-748.
9. Li ZB, Zhao SY, Zhao XG, He TS (2012) Leaching characteristics of steel slag components and their application incementitious property prediction. J Hazard Mater 200: 448-452.
10. Mombelli D, Mapelli C, Barella S, Gruttadauria A, Saout G L, Diaz EG. The efficiency of quartz addition on Electric Arc Furnace (EAF) carbon steel slag stability. J Hazard Mater 279: 586-596.
11. Sha F, Liu P, Ding YL (2021) Application investigation of high-phosphorus steel slag in cementitious material and ordinary concrete. J Mater Res Technol 11: 2074-2091.
12. Guan X, Wang JY, Xiao FP (2021) Sponge city strategy and application of pavement materials in 442sponge city. J Clean Prod 303: 127022.
13. Brand AS, Roesler JR (2015) Steel furnace slag aggregate expansion and hardened concrete properties. Cement & Concrete Comp 60: 1-9.
14. Anastasiou E, Georgiadis FK, Stefanidou M (2014) Utilization of fine recycled aggregates in concrete with fly ash and steel slag. Constr and Build Mater 50: 154-161.
15. Lai MM, Zou JJ, Yao BY, Ho JCM, Xin Z, et al. (2021) Improving mechanical behavior and microstructure of concrete by using BOF steel slag aggregate. Constr Build Mater 277: 122269.
16. Sharba AAK, Altemen AAA, Hason MM (2021) Shear behavior of exploiting recycled brick waste and steel slag as an alternative aggregate for concrete production. Materials Today: Proceedings 42: 2621-2628.
17. Thamali P, James MG, Prasanna EK, Jinadasa AG (2019) Taxonomy of influential factors for predicting pollutant first flush in urban stormwater runoff. Water Res 166: 115075.
18. Nitendra P, Ravi Shankar AU, Mithun BM (2016) Durability studies on eco-friendly concrete mixes incorporating steel slag as coarse aggregates. J Clean Prod 129: 437-448.
19. Narayanan N, Milani SS, Omkar D (2010) Characterizing pore volume, sizes, and connectivity in pervious concretes for permeability prediction. Materials Characterization 61: 802-813.
20. Gregory WK, Bruetsch AP, Kevern JT (2013) Slip-related characterization of gait kinetics: Investigation of pervious concrete as a slip-resistant walking surface. Safety Science 57: 52-59.

21. Linoshka SP, Sangchul H (2016) Mix design and pollution control potential of pervious concrete with non-compliant waste fly ash. J Environ Manage 176: 112-118.

22. Lua GY, Wang H, Tom T, Liu PF, Zhang YQ, et al. (2020) *In-situ* and numerical investigation on the dynamic response of unbounded granular material in permeable pavement. Transp Geotech 25: 100396.

23. Wang HB, Li H, Dai Z (2019) Investigation on the mechanical properties and environmental impacts of pervious concrete containing fly ash based on the cement-aggregate ratio. Constr Build Mater 202: 387-395.

24. Runze CM, Chai J (2018) Research on the performance of sand-based environmental friendly water permeable bricks. Environ Earth Sci 113: 78-88.

25. Wang Q, Yan PY, Yang JW, Zhang B (2013) Influence of steel slag on mechanical properties and durability of concrete. Constr Build Mater 47: 1414-1420.

26. Zhang WD, Wang ZB, Zhang Y (2019) Experimental study on compressive properties and abrasion resistance of pervious recycled concrete. Concrete 3: 147-152.

27. Zhang J, Ma GD, Dai ZX, Ming RP, Cui XZ, et al. (2018) Numerical study on pore clogging mechanism in pervious pavements. J Hydro 565: 589-598.

28. Shigemitsu H, Zilola K, Morihiro H (2019) Construction of a nonlinear permeability model of pervious concrete and drainage simulation of heavy rain in a residential area. Results Mater 3: 100033.

29. Othman A, Somayeh N (2021) Pervious concrete mixture optimization, physical, and mechanical properties and pavement design: A review. J Clean Prod 288: 125095.

30. Rosangel OV, Lizárraga MC, Coronel O, Luis DLC, Alfredo BAG, et al. (2019) Effect of photocatalytic Fe_2O_3 nanoparticles on urban runoff pollutant removal by permeable concrete. J Environ Manage 242: 487-495.

31. Shigemitsu H, Zilola K, Morihiro H (2019) Construction of a nonlinear permeability model of pervious concrete and drainage simulation of heavy rain in a residential area. Results Mater 3: 100033.

32. Xue Z, Hui L, John TH, Xiao L, Ning X, et al. (2021) Purification effect on runoff pollution of porous concrete with nano-TiO_2 photocatalytic coating. Transportation Research Part D: Transport and Environment 10:103101.

33. GB/T50081-2002 (2002) Standard for test method of mechanical properties on ordinary concrete.

34. HJJ/T1. 35-2009 (2009) Technical specification for previous cement concrete pavement.

35. Pirnia PY, Duhaime F, Ethier Y, Dubé JS (2019) ICY: An interface between COMSOL multiphysics and discrete element code YADE for the modelling of porous media. Comput Geosci 123: 38-46.

36. Zhou SX, Han Z, Wei X, Wei YQ, Yu L (2018) Influence of Aggregate Contents and Volume of Inter facial Transition Zone on Chloride Ion Diffusion Properties of Concrete. J Build Mater 21: 351.

37. Ma GD (2019) Numerical Study on the Seepage Flow and Pore Clogging Mechanism of Pervious Concrete Pavement.

38. Yang X, Wang MZ (2021) Fractal dimension analysis of aggregate packing process: A numerical case study on concrete simulation. Constr Build Mater 270: 121376.

39. Cui XZ, Zhang J, Huang D, Jin Q, Hou F (2016) Experimental Simulation of Rapid Clogging of Pervious Concrete Pavement Under Effects of Rainstorm. China J High Trans 29: 7-19.

40. Lei G, Gu SH, Dong LF, Liao QZ, Xue L (2021) Particle plugging in porous media under stress dependence by Monte Carlo simulations. J Petrol Sci Eng 207: 109144.

41. Xie X, Jiang C, Lin CT (2019) Research on Clogging and Effectiveness of Restoration Measures of Permeable Concrete Pavement. Journal of China and Foreign Highway 39: 46-49.

42. Zhang JF, Zang HB, Zhang YB, Li GQ, Lai XW, et al. (2021) An integrated separating system constructed by laser-patterned commercially available materials towards oily domestic sewage. Colloids and Surfaces A: Physicochemical and Engineering Aspects 621: 126566.

43. Ma CY, Feng YC, Lin H, Deng JG, Li XR, et al. (2021) CFD-DEM investigation of blocking mechanism in pre-packed gravel screen. Eng Anal Bound Elem 132: 416-426.

44. Nan X, Wang ZK, Hou JM, Tong Y, Li B (2021) Clogging mechanism of pervious concrete: From experiments to CFD-DEM simulations. Constr Build Mater 270: 121422.

45. GB/T22235-2008 (2008) Determination for viscosity of liquids.

46. GB/T4472-2011 (2011) Determination of density and relative density for chemical products.

47. Lee JW, Yang E, Jang J, Yun TS (2021) Effect of clogging and cleaning on the permeability of pervious block pavements. Int J Pavement Eng 1884861.

48. Erfanul H, Abdul Aziz OI (2021) Climate and land cover change impacts on stormwater runoff in large-scale coastal-urban environments. Sci Total Environ 778: 146017.

49. Devi VS, Kumar MM, Iswarya N, Gnanavel BK (2020) Durability of Steel Slag Concrete under Various Exposure Conditions. Mater Today Proceed 22: 2764-2771.

50. Brezonik PL, Sadelmann TH (2002) Analysis and predictive models of stormwater runoff volumes, loads, and pollutant concentrations from watersheds in the Twin Cities metropolitan area, Minnesota, USA. Water Res 36: 1743-1757.

51. Gnecco I, Berretta C, Lanza LG (2005) Storm water pollution in the urban environment of Genoa, Italy. Atmos Res 77: 60-73.

52. Newman AP, Coupe SJ, Smith HG, Puehmeier T, Bond P (2008) Microbiology of pervious concrete pavements and brick pavements. Building Block & Block Building 1: 31-35.

53. GB/T11901-1989 (1989) Water quality- Determination of suspended substance- Gravimetric method.

54. HJ/828-2017 (2017) Water quality-Determination of chemical oxygen demand- Dichromate method.

55. HJ/535-2009 (2009) Water quality-Determination of ammonia nitrogen - Nessler reagent spectrophotometry.

56. Kayhanian M, Anderson D, Harvey JT (2012) Permeability measurement and scan imaging to assess clogging of pervious concrete pavements in parking lots. Journal of Environmental Management 95: 114-123.

57. Yin LL, Yu F, Qin Y, Yuan F, Wu P, et al. (2020) The device and method of using to simulate clogging of permeable concrete pavement and rainwater purification monitoring. China Patents.

58. Xuan N, Zekun W, Hou JM, Yu T, Bo L (2021) Clogging mechanism of pervious concrete: From experiments to CFD-DEM simulations. Constr Build Mater 270: 121422.

59. Zhu JM, Bin HZ, Wang ZY, Zhou FZ (2000) A Grev Evaluation Method of Measurement Result with Standard Uncertainty. J Huazllong Univ. of SciTech 28: 84-86.

60. Li L (2018) Experimental and Simulation Study on the Pore Clogging Mechanism of Permeable Pavement.